Cr Vaporisation and Oxidation Behaviour of SUS430 Stainless Steel in the Simulated Cathodic Environment of Solid Oxide Fuel Cells

Joelle Chia Wen Mah[1], Muhamad Isyraf Aznam[1], Andanastuti Muchtar[1, 2*], Mahendra Rao Somalu[1], Mariyam Jameelah Ghazali[2]

[1]Fuel Cell Institute, Universiti Kebangsaan Malaysia, 43600 Bangi, Selangor Darul Ehsan, Malaysia
[2]Department of Mechanical & Manufacturing Engineering, Faculty of Engineering and Built Environment, Universiti Kebangsaan Malaysia, 43600 Bangi, Selangor Darul Ehsan, Malaysia

Abstract

The migration of volatile Cr species from the metallic interconnects to the cathode material affects the long-term performance, stability, and durability of solid oxide fuel cells (SOFCs). This study aimed to elucidate the formation of oxide scale layer on a commercially available SUS430 stainless steel in a simulated cathodic environment of SOFCs. In addition, the effects of Cr vaporisation on the electrical properties of pelletised $La_{0.6}Sr_{0.4}Co_{0.2}Fe_{0.8}O_{3-\delta}$ (LSCF) cathode were determined. A dual-layer oxide scale consisting of Cr_2O_3 (inner layer) and $(Mn,Cr)_3O_4$ (outer layer) formed on the steel substrates subjected to 200 h of oxidation showed insignificant effects on electrical properties. The trace of $SrCrO_4$ and Cr_2O_3 species detected on the pelletised LSCF cathode confirmed Cr vaporisation from the steel substrates. An increment of approximately 38.8% in activation energy of the LSCF cathode was related to the formation of $SrCrO_4$ and Cr_3O_4 species that reduced the concentration of oxygen vacancies and catalytic activities in the LSCF. Therefore, SUS430 stainless steel can only be used as SOFC interconnect material after the Cr vaporisation phenomena are effectively suppressed.

Keywords: SUS430 stainless steel, interconnect, focused ion beam (FIB)-FESEM, energy dispersive spectroscopy (EDX), electrical properties

Article Info

Received 11th November 2019
Accepted 7th March 2020
Published 1st April 2020
*Corresponding author: Andanastuti Muchtar; e-mail: muchtar@ukm.edu.my

ISSN: 1823-7010, eISSN: 2600-7444

Introduction

Solid oxide fuel cells (SOFCs) are clean, quiet and highly efficient electrochemical devices that directly convert chemical energy into electricity without mechanical combustion. SOFCs have three main components, namely, anode, electrolyte, and cathode. An electrolyte sandwiched between anode and cathode is generally known as a single cell. The single cells are connected by interconnects to accumulate voltage output for various applications. However, the applications of SOFCs are constrained by their high operating temperature, that is, near 1000°C [1]. Researchers have attempted to reduce the operating temperature to the range of 600 °C to 800 °C by developing novel materials with high ionic conductivity and producing thin electrolyte layers [2,3]. In consequence of the reduced operating temperatures, metal alloys with good electrical conductivity, mechanical strength and manufacturability can be considered to replace the conventional ceramic interconnects. The selection criteria of potential interconnect materials are of the most stringent amongst all components [4–6]. Given that interconnects operate in cathodic and anodic environments, the potential metallic candidate must be chemically stable in both oxidizing and reducing conditions. Excellent oxidation resistance at elevated temperatures and compatible thermal expansion coefficient (TEC) with adjacent components are deemed important for the interconnects to withstand high operating temperatures. In addition, the metallic candidate must be electrically conductive to accumulate voltage output.

Al- and Cr-containing alloys fulfil most of the stringent criteria; however, Al-containing alloys, which form insulative Al_2O_3-scales at elevated temperature are disqualified [7]. Amongst Cr-containing alloys, Fe-Cr-based alloys, which are commonly known as stainless steel, have received considerable attention because of their TEC compatibility with adjacent electrodes. Cr-containing alloys form dual-layer oxide scales, consisting of Cr_2O_3 (inner layer) and $(Mn,Cr)_3O_4$ (outer layer) upon oxidation [8]. Thermodynamic instability in the cathodic environment forms volatile Cr species through the following reactions [5]:

$$2\ Cr_2O_{3\ (s)} + 3\ O_{2\ (g)} \leftrightarrow 4\ CrO_{3\ (g)} \quad (1)$$

$$2\ Cr_2O_{3\ (s)} + 3\ O_{2\ (g)} + 4\ H_2O_{\ (g)} \leftrightarrow 4\ CrO_3(OH)_{2\ (g)} \quad (2)$$

$$Cr_2O_{3\ (s)} + O_{2\ (g)} + H_2O_{\ (g)} \leftrightarrow 2\ CrO_2OH_{\ (g)} \quad (3)$$

Deposition of volatile Cr species at the triple-phase boundaries forms inactive $SrCrO_4$ and Cr_2O_3 layer and reduces active areas in the cathode, thereby decreases the ionic conductivity and catalytic activity in the cathode [9]. Considering that the formation of oxide scale and Cr vaporisation phenomena are influenced by the chemical compositions of stainless steel, research has been conducted on tailoring a suitable alloying composition for SOFC applications [10]. Despite developing novel alloying composition that involve high manufacturing cost, this study aimed to elucidate the potential of a commercially available SUS430 stainless steel as SOFC interconnects. Aside from the growth rate of oxide scales and their effects on the electrical properties of SUS430 stainless steel, the Cr vaporisation from the SUS430 stainless steel to the cathode and their effects to the performance of the cathode that is essential for achieving long-term stability of the SOFC is reported.

Materials and methods

Commercially available SUS430 stainless steel was used in this work, and its chemical compositions are shown in Table 1. All steel substrates (15 mm × 15 mm × 1 mm) were polished with sandpapers and cleaned using acetone prior to oxidation. The steel substrates were oxidised at 800 °C for 200 h using a vertical tube furnace (VSTF35-1100, LT Furnace). The formation of oxide scale was quantified by weighing the samples before and after the oxidation process. Focused ion beam field emission scanning electron microscopy (FIB-FESEM; Helios NanoLab G3 UC, FEI Company) coupled with energy dispersive spectroscopy (EDX) was employed for surface morphology and elemental analysis, respectively. The electrical properties of the oxidised SUS430 stainless steel were measured at 800 °C up to 200 h using a four-probe conductivity measuring system built on the basis of van der Pauw's technique [11]. Commercial $La_{0.6}Sr_{0.4}Co_{0.2}Fe_{0.8}O_{3-\delta}$ (LSCF) perovskite powder (KCeraCell Co., Ltd, South Korea) with the specific surface area range between 5 m^2/g and 10 m^2/g was used to pelletise a 20 mm-diameter LSCF cathode. The LSCF perovskite powders were pressed and sintered at 1350 °C for 2 h at a heating rate of 5 °C/min [12]. The pelletise LSCF cathode was attached to a steel substrate (Figure 1) and oxidised at 800 °C for 200 h. Cr vaporisation from the steel substrate to the surface of the LSCF cathode was detected and analysed using FESEM and X-ray diffractometer (XRD; D8-Advance; Bruker). The effects of volatile Cr species on the electrical properties of the pelletised LSCF cathode were determined using a four-probe conductivity measuring system.

Table 1: Chemical compositions of the SUS430 stainless steel used in this work.

Fe	Cr	C	O	Si	Ni	Mn	P
78.5	14.6	4.8	1.0	0.5	0.4	0.2	0.1

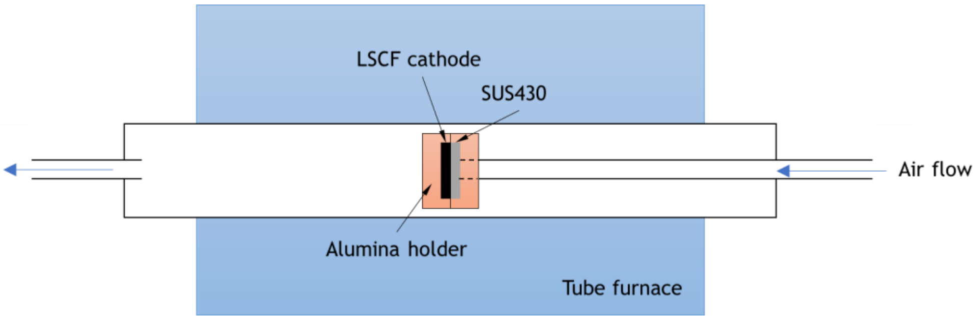

Figure 1: Set-up for the detection of Cr vaporisation in the simulated cathodic environment.

Results and discussion

Formation of an approximate 4 µm thick oxide layer was observed on the surface of the SUS430 steel substrate subjected to oxidation (Figure 2). Considering the brittle nature of the oxide scale, the cross-sectional view of the oxidised SUS430 stainless steel was examined through FIB-FESEM, without the need for sample preparation, such as grinding and polishing. Figure 3 shown an oxide scale layer of approximately 3 µm thick with microcracks and micropores observed at the substrate/oxide interface. The microcracks and micropores could further propagate and lead to delamination of the oxide scales under prolonged oxidation [13]. EDX line scan in Figure 3 confirmed a dual-layer oxide scale, consisting of Cr_2O_3 (zone B–C) and $(Mn,Cr)_3O_4$ spinel (zone C–D) on the steel substrates subjected to 200 h of oxidation. Fe is the main element in the steel substrate (zone A–B). The content of Fe was slowly diminished as the EDX line scan continue moving towards the oxide scale (zone B–C and zone C–D), indicating Fe does not contribute towards the formation and growth of oxide scales. The rapid formation of $(Mn,Cr)_3O_4$ spinel oxide scale was mainly because the absorption rate of Mn^{2+} ions was faster than that of Cr^{3+} ions. In the simulated cathode environment, Mn-content in the steel substrate was reduced into Mn^{2+}, which had a higher diffusion rate than Cr^{3+} ions. Thus, the Mn^{2+} ions acted as a nucleation agent that accelerates the crystallisation and growth of Cr_2O_3 and $(Mn,Cr)_3O_4$ spinel oxide scales [14,15]. The formation of $(Mn,Cr)_3O_4$ spinel is preferred for SOFC applications because of its low electrical resistance and Cr vaporisation rate compared with those of Cr_2O_3 [16].

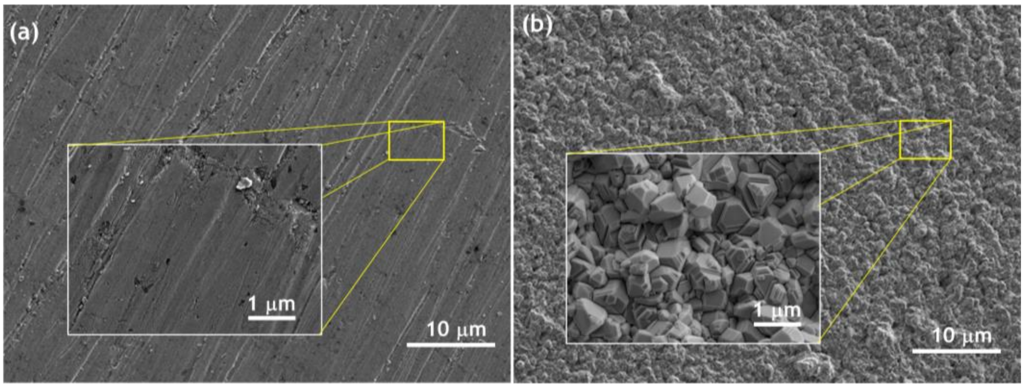

Figure 2: FESEM micrographs of SUS430 stainless steel (a) before and (b) after 200 h of oxidation.

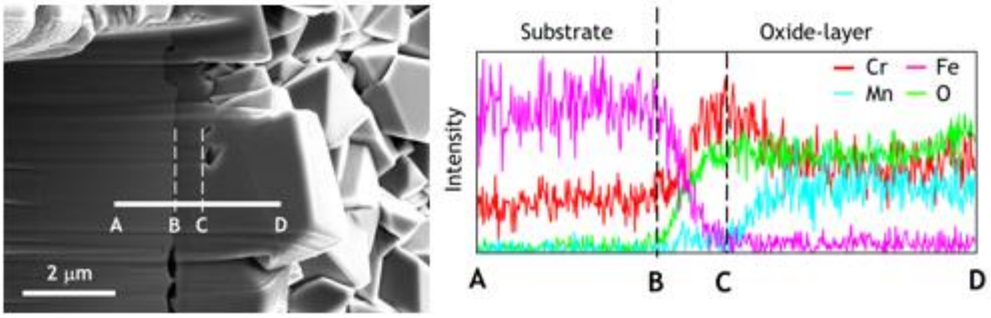

Figure 3: FIB-FESEM micrograph and EDX line scan of SUS430 stainless steel after 200 h of oxidation.

Changes on the surface morphology of the LSCF cathode exposed to SUS430 in a simulated cathode environment for 200 h were compared in Figure 4a and 4b. The growth of particulate and plate-like crystallites on the surface of the LSCF cathode after exposure were analysed and identified to be Cr_2O_3 and $SrCrO_4$, respectively (Figure 4c). Structural instability occurred when LSCF cathodes underwent prolonged high-temperature in a simulated cathode environment. The changes in the lattice structure of the LSCF cathode caused Sr-segregation, particularly SrO, which reacted with volatile Cr species from the steel substrates [17]. The formation of Cr_2O_3 and $SrCrO_4$ can be represented as follows [18]:

$$CrO_{3\,(g)} + SrO_{(s)} \rightarrow Cr\text{-}Sr\text{-}O_{(s)} \quad (4)$$

$$Cr\text{-}Sr\text{-}O_{(s)} + CrO_{3\,(g)} \rightarrow Cr_2O_{3\,(s)} \quad (5)$$

$$Cr\text{-}Sr\text{-}O_{(s)} + CrO_{3\,(g)} + SrO_{(s)} \rightarrow SrCrO_{4\,(s)} \quad (6)$$

Figure 5 shows the XRD pattern of LSCF cathode surface before and after exposure to the steel substrate in a simulated cathode environment. Comparing both diffraction patterns, additional peaks were observed in the LSCF cathode exposed to the steel substrate. The additional peaks matched well with Cr_2O_3 (ICDD card no. 01-074-1975) and $SrCrO_4$ (ICDD card no. 00-059-0308), confirms the formation of Cr_2O_3 and $SrCrO_4$ on the surface of LSCF cathode.

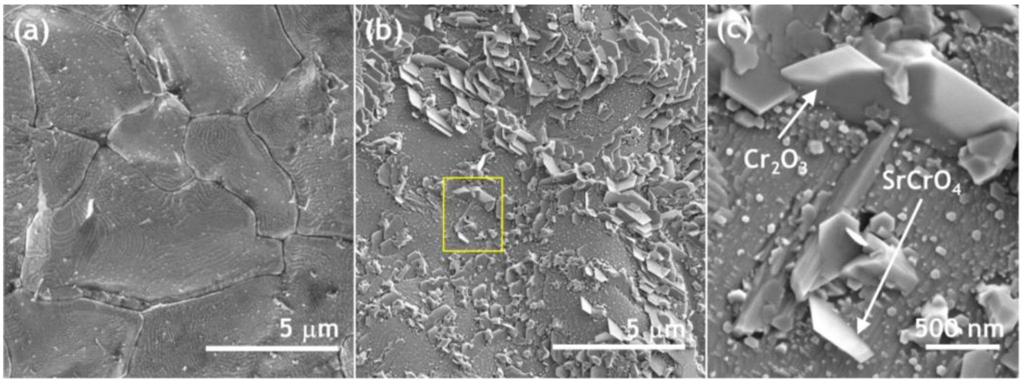

Figure 4: FESEM micrographs of the LSCF cathode surface (a) before and (b) after exposure to the steel substrate in a simulated cathode environment. (c) Crystalline Cr_3O_4 and $SrCrO_4$ on the LSCF cathode.

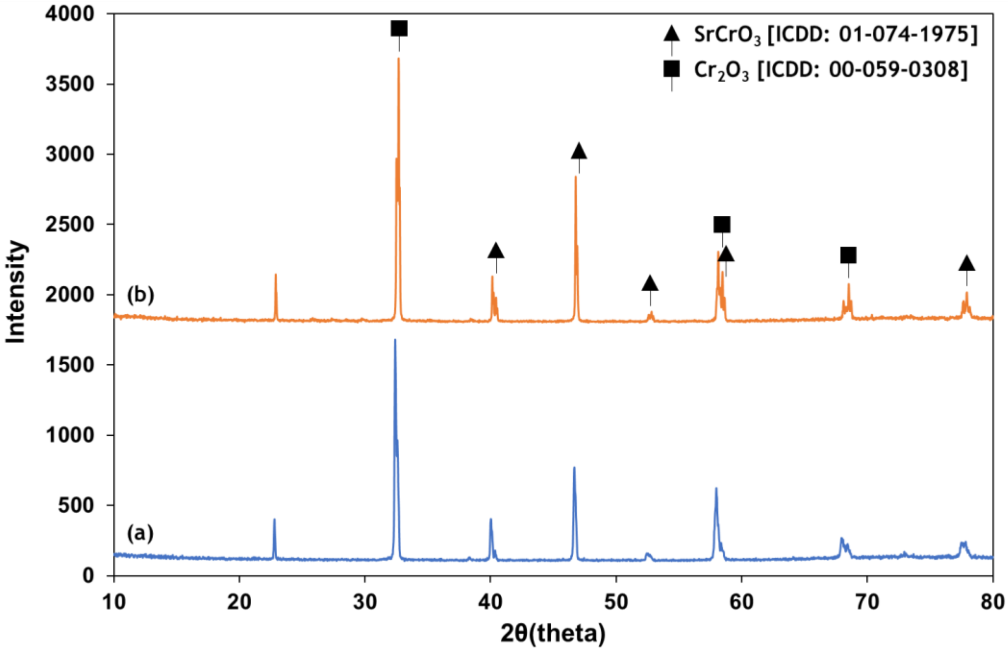

Figure 5: XRD pattern of the LSCF cathode surface (a) before and (b) after exposure to the steel substrate in a simulated cathode environment.

The oxidised steel substrate showed a stable electrical conductivity and area-specific resistance (ASR) at 800 °C up to 200 h, as depicted in Figure 6a. The electrical conductivity (higher than 100 $S.cm^{-1}$) and ASR (approximately 1.0×10^{-3} $\Omega.cm^2$) met the targeted values required for applications in SOFC. Therefore, SUS430 stainless steel has potential to be used as a SOFC interconnect. However, the low electrical conductivity of 1.76 and 13 $S{\cdot}cm^{-1}$ at 800 °C was measured on a 9 µm thick oxide scale, consisting of Cr_2O_3 (inner layer) and $(Mn,Cr)_3O_4$ spinel (outer layer) [19]. Prolonged oxidation may increase the thickness of the oxide scales, resulting in high ASR and low electrical conductivity. As such, further analysis on the growth rate of oxide scales is still in progress and will be reported elsewhere.

The conductivity of cathode materials determines the effectiveness of electron flow through them. LSCF cathode exhibits excellent mixed ionic–electronic conducting (MIEC) behaviour that enables rapid oxygen reduction at the cathode/electrolyte interface, and the triple-phase boundaries [20]. The electrical conductivity of LSCF cathode before and after exposure to the steel substrate in a simulated cathode environment was plotted as a function of temperature (Figure 6b). The total electrical conductivity of the as-sintered LSCF cathode was initially increased and decreased after a maximum value of 622 $S \cdot cm^{-1}$ at 600 °C. The increasing trend is in good agreement with the semiconductor and MIEC-type cathode materials that are influenced by the hopping mechanism of thermally activated small polarons [21,22]. Meanwhile, the decreasing trend is attributed to the increase in the concentration of oxygen vacancies in the LSCF cathode as the temperature increased. The decrease in the concentration of charge carriers and oxygen-content reduces the electronic contribution to the electrical conductivity at high operating temperatures [23]. After being exposed to the steel substrate, the electrical conductivity of the LSCF cathode was considerably decreased with a maximum value of 530 $S \cdot cm^{-1}$ at 700 °C. This phenomenon could be attributed to the deposition of the Cr_2O_3 and $SrCrO_4$ observed on the LSCF cathode surface, which has a significant effect on the oxygen-catalytic activity. Reactions between CrO_3 and SrO considerably increased the concentration of oxygen vacancies in the LSCF cathode and accelerated the depletion of oxygen and the concentration of charge carriers, resulting in decreased electrical conductivity [24]. The LSCF cathode before and after exposure to the steel substrate in a simulated cathode environment exhibited near-linear fits in the Arrhenius plot (Figure 6b) and was consistent with the semiconducting behaviour discussed earlier. The activation energy of the electron conductions was calculated from the slope of the linear fits. The increase in the activation energy of the electron conduction from 0.7762 eV to 1.0758 eV, could be attributed to the deposition of Cr_2O_3 and $SrCrO_4$ that suppressed the catalytic activity. Thus, the deposition of catalytically inactive Cr_2O_3 and $SrCrO_4$ that may result in cell degradation and affect the long-term stability of SOFC is unfavourable.

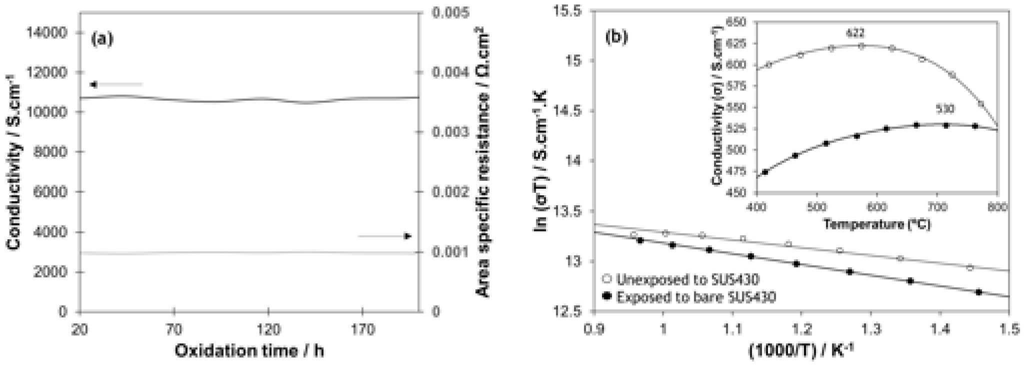

Figure 6: (a) Electrical conductivity and area-specific resistance of the oxidised SUS430 stainless steel. (b) Arrhenius plot and temperature-dependent electrical conductivity (insert) of the LSCF cathode before and after exposure to the steel substrate in a simulated cathode environment.

Conclusion

SUS430 stainless steel, which demonstrates good oxidation resistance and excellent electrical conductivity, is suitable to be used as SOFC interconnects. However, the rapid growth of oxide scales leads to Cr vaporisation from the interconnects onto LSCF cathode and forms inactive catalytic layer that contains Cr_2O_3, $SrCrO_4$ and $CrCoO_3$. Consequently, reduction at the cathode is retarded and the cell performance deteriorates. To ensure long-term stability and durability of the SOFC for realistic applications, protective coatings that could suppress outward diffusion of the volatile Cr species, at the same time, maintain good oxidation resistance and electrical performance, deem essential.

Acknowledgment

This work was funded by the FRGS Grant no: FRGS/1/2018/TK10/UKM/01/1. The authors would also like to thank the Centre for Research and Instrumentation Management, UKM for the use of their excellent testing equipment.

Author Contributions

All authors contributed toward data analysis, drafting and critically revising the paper and agree to be accountable for all aspects of the work.

Disclosure of Conflict of Interest

The authors have no disclosures to declare.

Compliance with Ethical Standards

The work is compliant with ethical standards.

References

[1] Mahmud L S, Muchtar A and Somalu M R (2017) Challenges in fabricating planar solid oxide fuel cells: A review. *Renew. Sustain. Energy Rev.* 72 105–116

[2] Zakaria Z, Awang Mat Z, Abu Hassan S H and Boon Kar Y (2020) A review of solid oxide fuel cell component fabrication methods toward lowering temperature. *Int. J. Energy Res.* 44 594–611

[3] Anwar M, Muhammed A, Abdalla A, Somalu R and Muchtar A (2017) Effect of sintering temperature on the microstructure and ionic conductivity of Ce0.8Sm0.1Ba0.1O2-δ electrolyte. *Process. Appl. Ceram.* 11 67–74

[4] Qi Q, Liu Y and Huang Z (2015) Promising metal matrix composites (TiC/Ni–Cr) for intermediate-temperature solid oxide fuel cell (SOFC) interconnect applications. *Scr. Mater.* 109 56–60

[5] Mah J C W, Muchtar A, Somalu M R and Ghazali M J (2017) Metallic interconnects for solid oxide fuel cell: A review on protective coating and deposition techniques. *Int. J. Hydrogen Energy* 42 9219–29

[6] Irshad M, Siraj K, Raza R, Ali A, Tiwari P, Zhu B, Rafique A, Ali A, Kaleem Ullah M and Usman A (2016) A Brief Description of High Temperature Solid Oxide Fuel Cell’s Operation, Materials, Design, Fabrication Technologies and Performance. *Appl. Sci.* 6 75

[7] Shaigan N, Qu W, Ivey D G and Chen W (2010) A review of recent progress in coatings, surface modifications and alloy developments for solid oxide fuel cell ferritic stainless steel interconnects. *J. Power Sources* 195 1529–42

[8] Sachitanand R, Sattari M, Svensson J-E E and Froitzheim J (2013) Evaluation of the oxidation and Cr evaporation properties of selected FeCr alloys used as SOFC interconnects. *Int. J. Hydrogen Energy* 38 15328–34

[9] Hua B, Pu J, Lu F, Zhang J, Chi B and Jian L (2010) Development of a Fe–Cr alloy for interconnect application in intermediate temperature solid oxide fuel cells. *J. Power Sources* 195 2782–8

[10] Garcia-Fresnillo L, Niewolak L, Quadakkers W J and Meier G H (2018) Influence of Alloying Elements on the Behavior of Different Ferritic Steels as Candidate Materials for SOFC Interconnect. *Oxid. Met.* 89 61–80

[11] Baharuddin N A, Muchtar A, Somalu M R, Kalib N S and Raduwan N F (2018) Synthesis and characterization of cobalt-free SrFe0·8Ti0·2O3-δ cathode powders synthesized through combustion method for solid oxide fuel cells. *Int. J. Hydrogen Energy.* 44 30682–30691

[12] Muhammed Ali S A, Anwar M, Ashikin N, Muchtar A and Somalu M R (2018) Influence of oxygen ion enrichment on optical, mechanical, and electrical properties of LSCF perovskite nanocomposite. *Ceram. Int.* 44 10433–42

[13] Brylewski T, Kucza W, Adamczyk A, Kruk A, Stygar M, Bobruk M and Dąbrowa J (2014) Microstructure and electrical properties of Mn1+xCo2−xO4 (0⩽x⩽1.5) spinels synthesized using EDTA-gel processes. *Ceram. Int*. 40 13873–82

[14] Jo K H, Kim J H, Kim K M, Lee I S and Kim S J (2015) Development of a new cost effective Fe-Cr ferritic stainless steel for SOFC interconnect. *Int. J. Hydrogen Energy* 40 9523–9

[15] Jiang S P, Zhang S and Zhen Y D 2005 Early interaction between Fe-Cr alloy metallic interconnect and Sr-doped LaMnO3cathodes of solid oxide fuel cells J. Mater. Res. 20 747–58

[16] Falk-Windisch H, Svensson J E and Froitzheim J (2015) The effect of temperature on chromium vaporization and oxide scale growth on interconnect steels for Solid Oxide Fuel Cells. *J. Power Sources* 287 25–35

[17] Jiang S P, Zhen Y D, Zhang S, Tok A I Y and Wu P (2006) An Electrochemical Method to Assess the Chromium Volatility of Chromia-Forming Metallic Interconnect for SOFCs. *J. Electrochem. Soc.* 153 A2120

[18] Jiang S P and Chen X (2014) Chromium deposition and poisoning of cathodes of solid oxide fuel cells - A review. *Int. J. Hydrogen Energy* 39 505–31

[19] Sakai N, Horita T, Xiong Y P, Yamaji K, Kishimoto H, Brito M E, Yokokawa H and Maruyama T (2005) Structure and transport property of manganese-chromium-iron oxide as a main compound in oxide scales of alloy interconnects for SOFCs. *Solid State Ionics* 176 681–6

[20] Sun C, Hui R and Roller J (2010) Cathode materials for solid oxide fuel cells: A review. *J. Solid State Electrochem*. 14 1125–44

[21] Xu Q, Huang D ping, Zhang F, Chen W, Chen M and Liu H (2008) Structure, electrical conducting and thermal expansion properties of La0.6Sr0.4Co0.8Fe0.2O3-δ-Ce0.8Sm0.2O2-δcomposite cathodes. *J. Alloys Compd.* 454 460–5

[22] Da Conceião L, Silva A M, Ribeiro N F P and Souza M M V M (2011) Combustion synthesis of La0.7Sr0.3Co0.5Fe0.5O3(LSCF) porous materials for application as cathode in IT-SOFC. *Mater. Res. Bull*. 46 308–14

[23] Muhammed M A, Anwar M, Raduwan N F, Muchtar A and Somalu M R (2018) Optical, mechanical and electrical properties of LSCF–SDC composite cathode

prepared by sol–gel assisted rotary evaporation technique. *J. Sol-Gel Sci. Technol*. 86 1–12

[24] Oh D, Armstrong E, Jung D, Kan C and Wachsman E (2009) Mechanistic Understanding of Cr Poisoning on La0.6Sr0.4Co0.2Fe0.8O3-δ (LSCF). *ECS Trans.* 25 2871–9